Food Hydrocolloids 45 (2015) 72–82

Contents lists available at ScienceDirect

Food Hydrocolloids

journal homepage: www.elsevier.com/locate/foodhyd

Effects of salt and sugar addition on the physicochemical properties and nanostructure of fish gelatin

Li Cheng Sow [a, b], Hongshun Yang [a, b, *]

[a] Food Science and Technology Programme, c/o Department of Chemistry, National University of Singapore, 117543, Singapore
[b] National University of Singapore (Suzhou) Research Institute, 377 Lin Quan Street, Suzhou Industrial Park, Suzhou, Jiangsu 215123, PR China

ARTICLE INFO

Article history:
Received 21 August 2014
Accepted 21 October 2014
Available online 13 November 2014

Keywords:
Fish gelatin
Sodium chloride
Sucrose
Atomic force microscopy (AFM)
Nanostructure
Fourier transform infrared spectroscopy (FTIR)

ABSTRACT

Application of fish gelatin as a food component in replace of mammalian sources has attracted attentions recently. However, physicochemical properties of fish gelatin might be affected by other food components thus affecting its application. To determine whether and how sugar and salt components in food affect the physicochemical properties of fish gelatin, nanostructure of tilapia fish gelatin was studied by atomic force microscopy (AFM) with the secondary structure investigated by Fourier transform infrared (FTIR) spectroscopy. The results indicated that 1.5% NaCl addition led to a loss in molecular order in secondary structure which was accompanied with reducted gel strength; however, addition of 1.5% sucrose did not affect physicochemical and structural properties of fish gelatin. Fish gelatin possessed heterogeneous nanostructure including spherical aggregates, ring like structure, short and long rods as well as continuous fibre network. Incorporation of NaCl with fish gelatin increased diameter of spherical aggregates to more than two folds of control. These data suggest that addition of NaCl reduced gel strength through inducing large nano-aggregates, which could be at improper alignment that prevented the formation of a rigid gel. Interestingly, the fish skin gelatin studied here showed good storage stability over 30 days of storage at 4 °C. Sodium chloride affects fish gelatin's nanostructure and physicochemical properties more than sucrose at the same concentration.

1. Introduction

Currently, about 98.5% of world gelatin production is extracted from cattle hides, beef bones and pork skin (Karim & Bhat, 2009). Applications of gelatin from pork and beef byproducts have religious restrictions as well as food safety concern because these gelatin may be contaminated by pathogenic vectors such as prions from the diseased animal (Karim & Bhat, 2009). Due to these concerns alternative sources of gelatin such as gelatin extracted from fish would be valuable and has attracted many interests in recent years.

To expand the application of fish gelatin in food, the understanding of how properties of fish gelatin are impacted by common food components such as salt and sugar is important. In food application, both salt and sugar are common solutes present in most of the formulations. The level of sugar present in food could range from high in dessert and confectionary (more than 10%) to a low concentration as what exists in pasta sauces, soups, meat and ham (less than 5%) (USDA, 2013). While the addition of salt is often self-limited due to the intense salty taste, the concentration of salt in restaurant food, meals and fast food could range from less than 0.1% to as high as 2.15% (USDA, 2013).

The effect of solute addition on gelatin has been studied in terms of physicochemical properties. The solutes that have been studied include electrolytes such as NaCl (Haug, Draget, & Smidsrød, 2004), $MgCl_2$ and $MgSO_4$ (Sarabia, Gomez-Guillen, & Montero, 2000), $CaCl_2$ and phosphate salt (Kaewruang, Benjakul, Prodpran, Encarnacion, & Nalinanon, 2014), and non-electrolytes such as sucrose (Choi, Lim, & Yoo, 2004; Choi & Regenstein, 2000; Koli, Basu, Nayak, Kannuchamy, & Gudipati, 2011). It was proposed that electrolytes such as salts could affect gelatin via modification of the electrostatic forces and formation of salt bridges (Kaewruang et al., 2014), while non-electrolyte such as sugars could affect gelatin gel properties due to the hydration effect or stabilising of hydrogen bond (Choi et al., 2004). However the observed changes in physical properties of fish gelatin due to solute addition have not been fully understood especially the underlying mechanism.

* Corresponding author. Food Science and Technology Programme, c/o Department of Chemistry, National University of Singapore, 117543, Singapore. Tel.: +65 65164695; fax: +65 67757895.
E-mail address: chmynghs@nus.edu.sg (H. Yang).

http://dx.doi.org/10.1016/j.foodhyd.2014.10.021
0268-005X/

As a thermo reversible gel, gelation of gelatin is induced by transiting coil to helix below gelling temperature, the individual α-chain could be partially renatured to triple helix like that occurred in collagen, which serves as junction zones cross-linked by flexible peptide chains (Haug et al., 2004). The structure of gelatin is affected by distribution of polypeptide fragments when collagen is partially hydrolysed into gelatin, the subsequent aggregation of the peptide fractions as well as the inherent amino acid composition (Yang, Wang, Regenstein, & Rouse, 2007). Structural studies of gelatin have been conducted using different methodologies. The secondary structure of gelatin such as the relative proportion of helix and coil could be determined using Fourier transform infrared spectroscopy (FTIR) (Ahmad & Benjakul, 2011; Muyonga, Cole, & Duodu, 2004) and circular dichroism (Giménez, Turnay, Lizarbe, Montero, & Gómez-Guillén, 2005). The X-ray diffraction analysis has been used to determine the fibril distribution (Zhang, Xu, & Wang, 2011). However, these methods provide a sample-wide average information of gelatin structure (Feng, Lai, & Yang, 2014; Yang & Wang, 2009).

Atomic force microscope (AFM) has been successfully applied to investigate detailed nanostructure of fish gelatin that had not been sophisticatedly prepared (Yang & Wang, 2009; Yang, Wang, Regenstein, et al., 2007). Nanostructure of colloid is closely correlated to its physical properties including stability, diffusivity and permeability (Díaz-Calderón, Caballero, Melo, & Enrione, 2014).

The objectives of this study were to investigate whether and how the addition of salt and sugar at low concentration (1.5%, w/w) affect the physicochemical properties of fish gelatin. The physicochemical properties including texture and viscosity were analysed together with gelatin's secondary structure and nanostructure in order to elucidate the underlying mechanism of physicochemical property changes. These results could be extended to understand the effects of other components on the properties of fish gelatin.

2. Materials and methods

2.1. Sample preparation

Commercial tilapia fish gelatin (180 Bloom) was purchased from Jiangxi Cosen Biology Co., Ltd (Yingtan, Jiangxi, China). The gelatin contained 83.14% protein, 0.68% ash, 9.12% moisture and 7.06% of other substances. Three groups of samples were prepared, i.e. control sample containing fish gelatin only (FG), fish gelatin with NaCl (FGN), fish gelatin with sucrose (FGS). Fish gelatin solution (6.67%, w/w) was prepared following the method modified from Yang and Wang (2009). Gelatin was soaked in distilled water until completely swollen, heated and stirred in a 65 °C water bath for 10 min. Sodium nitrite was added into the gelatin solution as antimicrobial agents at level of 0.1% to prevent microbial spoilage. To examine the effect of added solutes on gelatin gels, sucrose and NaCl were dry blended with fish gelatin powder before hydration, the final concentration of the solutes in gelatin solution was at 1.5% w/w. After heating, the solutions were immediately filled into a small cylindrical-shaped flat bottom plastic container (31 mm diameter × 25 mm height). The solution was then stored at 10 ± 2 °C for 17 ± 1 h to ensure the gels had matured evenly, and considered as sample at day 0. Subsequent storage of the gelatin gels were carried out at 4 ± 1 °C for 30 days.

2.2. Gel strength & texture profile analysis (TPA)

Day 0 results were obtained immediately after gel maturation at 10 °C for 17 ± 1 h. For subsequent storage time, gelatin gels were removed from the refrigerators and equilibrated to 10 °C for at least 0.5 h in cold water bath prior to measurement. Gel strength was determined by a TA.XT2-i Texture Analyser (Stable Micro System, Goldaming, Surrey, UK). For gel strength analysis, a 0.5″ radius cylinder probe (P/0.5R) was used to penetrate 4 mm into the gelatin gel at a speed of 0.5 mm/s. Gel strength of gelatin was defined as the maximum force required to penetrate 4 mm of gel, and recorded in unit of g (Yang & Wang, 2009). While for TPA, the gel sample was subject to two cycle compression to 40% of its original height with a flat cylindrical probe (47 mm). The detailed test settings were pre-test speed: 1.0 mm/s; Test speed: 0.5 mm/s; Target mode: Distance; Distance of compression: 12.4 mm (40% of original gel height); Time: 10.0 s; Trigger type: Auto (Force); Trigger Force: 0.05 N; Tare mode: Auto; and Advanced Options: On. Hardness, cohesiveness, springiness and chewiness were calculated from TPA curve according to the definition as described in Yang, Wang, Jiang, et al. (2007).

2.3. Viscosity

Fish gelatin gel was melt in a 60 °C water bath for less than 1 h. The viscosity of gelatin solution was measured at 60 °C using a Brookfield DV II + viscometer (Brookfield Engineering, Middleboro, MA, USA) equipped with No. 1 spindle at 100 rpm rotation. The gelatin solution was filled in a sample holding tube that was connected with circulated water bath which was set at 60 °C to maintain the temperature during measurement.

2.4. Fourier transform infrared (FTIR) spectroscopy

The gelatin gels were taken out after respective storage time and freeze dried for FTIR analysis. The freeze dried gelatin was milled into powder and grinded with KBr powder (Merck KGaA, Damstadt, Germany) at a ratio of 3 mg of gelatin to 100 mg of KBr. The KBr powder was stored and dried at 120 °C to eliminate moisture absorpted. The pellet was examined using a Spectrum One FTIR spectrometer (PerkinElmer, Waltham, MA, USA). The scan was conducted between 4000 and 450 cm^{-1} with resolution of 4 cm^{-1}. The background spectrum was collected before each scan. For each sample, at least triplicate of spectra were obtained. The spectra of a same sample with an average of 32 scans were smoothened, baseline corrected, normalised and averaged for qualitative interpretation of spectra.

For peak height and location of peak, amide A, amide I, amide II and amide III were selected for quantitative measurement of maximum peak height and location (wavenumber) using Spectrum software (version 5.0.1, PerkinElmer). Baseline of each band was defined by software, and the corrected peak height was taken as the absorbance difference from the peak to the baseline.

Deconvolution of amide I was also studied for further quantitative analysis. The spectra region between 1720 and 1590 cm^{-1} was selected as amide I band, of which each unprocessed spectra were cut and baseline corrected. Fourier self deconvolution was performed using the Spectrum software (version 5.0.1, PerkinElmer) with line narrowing factor, gamma, set at 1.0 and the smoothing length width set at 50%–60% by using Bessel type smoothing function. The deconvoluted amide I band was then fitted using Origin Pro 9 (OriginLab, Northampton, MA, USA). Gaussian curve fitting function was employed, using procedure described in Byler and Susi (1986) with slightly adjustment. The iteration was performed until the fit converged. The final fitting quality of the curve had corrected R^2 value greater than 0.99. The component peaks identified after deconvolution and curve fitting were compared to literature; the percent contribution of specific component was calculated by the area of the component peak divided by the total area of amide I band before deconvolution (Byler & Susi, 1986).

2.5. Atomic force microscopy (AFM)

Before AFM imaging, gelatin gel samples were thawed at room temperature. The sample preparation followed the method for AFM imaging at high gelatin concentration (Yang & Wang, 2009). The thawed samples were melted in a 60 °C water bath and stirred using a vortex mixer until homogenous. About 10 μl of each solution was pipetted rapidly onto a piece of freshly cleaved mica sheet that sticked onto a 15 mm diameter AFM specimen disc. A camera blower was used to facilitate the distribution of solution on mica sheet, which was then kept in a desiccator for at least 24 h before imaging.

Characterisation of gelatin nanostructure was carried out by TT-AFM (AFM workshop, Signal Hill, CA, USA) that was equipped with a Sensaprobe TM190-A-15 tip (Applied Nanostructures, Mountain View, CA, USA) at resonance frequency: 145–230 KHz; force constant: 25–95 N/m and a Z scanner about 0.2–0.4 Hz. A vibration mode was selected and the imaging was carried out under ambient air and temperature. The images obtained were analysed using Gwyddion software (http://gwyddion.net). Bright and dark areas in the image represented peak and troughs of the sample. To improve quality of image, reduction of electronic noise in raw data was performed by the software without flattening correction. Images were displayed in both height mode and error signal mode. The dimensions of aggregates were measured using the line profile extraction function of the Gwyddion software (Yang & Wang, 2009; Yang, Wang, Regenstein, et al., 2007).

2.6. Statistical analysis

All the experiments were repeated at least three times with at least triplicate of samples within each run. The results were reported as mean ± standard deviation. The difference in the results among different groups were determined using ANOVA ($P < 0.05$) and Duncan's multiple range test, performed by SAS software (version 9.2, Cary, NC, USA). For AFM, dozens of parallel imaging were conducted to obtain reliable, representative and statistically valid results.

3. Results and discussion

3.1. Gel strength and TPA

The effect of storage time and solute addition on gel strength and TPA of fish gelatin is presented in Table 1. In general, a higher value of gel strength and TPA parameters indicates a stronger gel (Yang, Wang, Jiang, et al., 2007). Gelatin is commercially characterized by the value of bloom, which is a specific unit of gel strength measured at 10 °C according to a specific protocol that requires preparation of gelatin at 6.67% concentration and maturation at 2–10 °C for 17 ± 1 h (Zhou, Mulvaney, & Regenstein, 2006).

Sharp increase of fish gelatin (FG) gel strength was observed from day 0 to day 5, the increasing trend of gel strength was continued up to day 15 and became stable until the end of 30 days storage. The increment of gel strength after 30 days of storage was about 152% of the original gel strength. The increased gel strength agreed with the study of Arnesen and Gildberg (2007) who found that the gel strength of salmon (108 Bloom), cod (71 Bloom) and porcine gelatin (216 Bloom) stored at 10 °C increased up to 7 days. The stronger gel could be due to the renaturation of triple helix, increased crosslink of junction zones, as well as the formation of hydrogen bond between hydroxylated amino acid and incorporated water (Arnesen & Gildberg, 2007).

Addition of 1.5% NaCl into fish gelatin gel (FGN) resulted in reduction of gel strength compared to the control sample containing fish gelatin only (FG) and the fish gelatin containing 1.5% sucrose (FGS). Addition of NaCl increased the ionic strength of solution and this could result in reduction of electrostatic bridges of α-chain due to the screening off effect of the short range electrostatic interactions (Haug et al., 2004). On the other hand, Choi and Regenstein (2000) proposed that the reduction of gel strength is due to the capability of NaCl to break hydrogen bond and interfere hydrophobic interaction. As a consequence, the addition of saline ion altered the formation of initial nucleation site (junction zone) and subsequent protein conformation, which stopped the formation of a rigid gel (Sarabia et al., 2000). Moreover, Choi and Regenstein (2000) found decreased gel strength was accompanied with increased NaCl addition from 0 % to 14 % (w/w) into gelatins from different sources including pork skin (100 Bloom and 300 Bloom), fish skin (225, 200 and 190 Bloom) and pork bone (230 Bloom).

The FGS sample had a decreased initial gel strength at day 0 compared to FG; however, FGS gel strength increased over the storage to a level that its final gel strength was comparable to FG. The lower initial gel strength of FGS than FG could be explained that addition of sucrose retarded the gelation time due to competition of water of hydration between gelatin and sucrose (Choi et al., 2004). Non-electrolytes such as sugars and glycerol increased the gel strength of gelatin due to the ability of sucrose to stabilise hydrogen bond (Koli et al., 2011). However, there is also opposite opinion that addition of sucrose decreased gel strength by weakening gelatin–gelatin interaction and increasing distance between entangled point therefore reducing the amount of available junction zone (Choi et al., 2004). In the current study no improvement of gel strength was found when 1.5% of sucrose was added into the fish gelatin. This may be due to differences in gelatin sources as well as sucrose concentration. In the current study, 1.5% of sucrose was added into tilapia fish skin gelatin while in other studies, increased gel strength was observed when 2%–14% of sucrose was used in commercial pork and fish gelatin (Choi & Regenstein, 2000). However, while when 7.5% (w/v) of sucrose was added into tiger toothed croaker (*Otolithes ruber*) gelatin (170 Bloom), gel strength decreased from 170.00 g to 150.50 g (Koli et al., 2011).

Similar to gel strength, the hardness and chewiness also increased with the length of storage. However, the increment only last for 10 days. The hardness value indicates the initial strength required to compress the gel while chewiness is related to the work required to masticate the food into a ready-to-swallow state (Yang, Wang, Jiang, et al., 2007). Thus the increased hardness and chewiness of fish gelatin suggests a firmer texture of food. The springiness and cohesiveness of fish gelatin throughout the storage at 4 °C were at a high and stable level. No significant effect on the springiness and cohesiveness of gelatin was found when solute was added, which indicated tilapia fish skin gelatin is strong and able to reform the structure after compression (Yang, Wang, Jiang, et al., 2007).

3.2. Viscosity

Effects of sucrose and sodium chloride addition on the viscosity of fish gelatin during storage are shown in Table 1. FGN and FGS had higher viscosity than FG at day 0. However, the viscosity of FGN and FGS was decreased from day 0 to day 5 and became comparable with FG. Following day 5, the viscosity remained stable up to 30 days. All samples determined here had higher viscosity than the commercial pig and beef gelatins that had viscosities between 2 cP to 8 cP and medium blooms (150–200 bloom) (Johnston-Banks, 1990). The viscosity of gelatin is more affected by molecular weight of gelatin and the distribution of molecular weight, the addition of solutes and storage of gelatin gel did not altered the

Table 1
Gel strength, TPA parameters (hardness, springiness, cohesiveness, chewiness) and viscosity of fish gelatin only (FG) and fish gelatin added with 1.5% NaCl (FGN) and 1.5% sucrose (FGS) over 30 days of storage at 4 °C.

Time/day	Gel strength/g			Hardness/g			Springiness		
	FG	FGN	FGS	FG	FGN	FGS	FG	FGN	FGS
0	165 ± 11^{aE}	137 ± 7^{cE}	145 ± 9^{bE}	1669 ± 235^{aE}	1479 ± 206^{bD}	1727 ± 261^{aD}	0.91 ± 0.04^{aA}	0.92 ± 0.02^{aA}	0.92 ± 0.03^{aA}
5	202 ± 16^{aD}	176 ± 11^{bD}	205 ± 13^{aD}	2228 ± 314^{abD}	2066 ± 285^{bC}	2302 ± 274^{aC}	0.91 ± 0.05^{aA}	0.92 ± 0.03^{aAB}	0.92 ± 0.04^{aA}
10	224 ± 15^{aC}	188 ± 9^{bC}	217 ± 12^{aC}	2396 ± 370^{abCD}	2193 ± 375^{bBC}	2551 ± 371^{aB}	0.91 ± 0.05^{aA}	0.90 ± 0.03^{aBC}	0.91 ± 0.04^{aA}
15	238 ± 17^{aAB}	202 ± 13^{bB}	232 ± 12^{aB}	2500 ± 261^{aBC}	2266 ± 281^{aABC}	2659 ± 304^{bAB}	0.90 ± 0.04^{aA}	0.90 ± 0.03^{aC}	0.91 ± 0.03^{aA}
20	235 ± 13^{aBC}	203 ± 10^{cB}	227 ± 8^{bB}	2492 ± 267^{abBC}	2385 ± 316^{bAB}	2603 ± 311^{aAB}	0.89 ± 0.04^{aA}	0.91 ± 0.03^{aABC}	0.90 ± 0.03^{aA}
25	248 ± 20^{aAB}	209 ± 12^{bAB}	243 ± 15^{aA}	2699 ± 434^{aAB}	2419 ± 399^{bA}	2632 ± 270^{abAB}	0.89 ± 0.04^{aA}	0.91 ± 0.03^{aABC}	0.90 ± 0.03^{aA}
30	251 ± 18^{aA}	213 ± 11^{bA}	247 ± 14^{aA}	2849 ± 331^{aA}	2457 ± 249^{bA}	2789 ± 270^{aA}	0.90 ± 0.04^{aA}	0.91 ± 0.03^{aABC}	0.90 ± 0.03^{aA}

*Within each row, means with different lowercase letters are significantly different ($P < 0.05$) among different groups. Within each column, means with different capital letters are significantly different among different time points ($P < 0.05$).

molecular weight of gelatin thus no significant changes in viscosity were observed (Gudmundsson & Hafsteinsson, 1997; Zhou et al., 2006). The current result is consistent with that reported, which indicated other factors such as concentration of gelatin solution and temperature (Gudmundsson, 2002), pH of gelatin solution, and measurement technique also affect its viscosity (Jamilah & Harvinder, 2002). This may explain the discrepancy of viscosity values found. A previous report indicated that viscosity of gelatin affected the properties of gel, such that high viscosity gelatin solution resulted in short and brittle gel, while low viscosity gelatin solution led to tough and extensible gel (Zhou et al., 2006). However, our current results did not show strong correlation between gelatin texture and viscosity.

3.3. FTIR spectroscopy

To investigate how solute addition affects gelatin properties, FTIR spectra were analysed. Qualitative comparison of FTIR spectra was based on the averaged spectra of samples, as shown in Fig. 1. Six regions of the spectra, including amide A, amide B, amide I, amide II, amide III and the fingerprint region, were investigated. The details of the location and assignment of each peak were listed in Table 2.

The major amide bands (amide A, B, I, II, III) were present in all spectra with some variations in wavenumber and peak height. The tendency of amide A to join with amide B and the CH_2 stretch bands were observed in all spectra, which may be due to the dimeric intermolecular association of carboxylic group (Muyonga et al., 2004). The FGS spectra could be differentiated from FG and FGN based on the difference in the fingerprint region, in particular the peaks at 1056 ± 2 cm^{-1}, 997 ± 1 cm^{-1} and 927 ± 2 cm^{-1}, the characteristic peaks of sucrose in FTIR spectra associated with C–O skeletal stretch (Garrigues, Akssira, Rambla, Garrigues, & de la Guardia, 2000). Storage length of fish gelatin samples did not cause significant difference in the spectra in term of the location of the bands and peaks. In general, the FTIR spectra in Fig. 1 were similar to the spectra observed by Pranoto et al. (2007) for tilapia skin gelatin.

Compared to FG and FGS, absorption intensity of overall FTIR spectra of FGN samples was decreased. To compare absorption intensity, the peak height of the four amide bands (Amides A, I, II and II) were quantitatively measured and compared (Fig. S1). The amount of gelatin in KBr pellet was controlled to ensure the same amount of gelatin was used for FTIR measurement for each sample, as the concentration of gelatin in the pellet affected the absorption intensity. The average location of amide A band for all samples was close to the free NH stretching frequency at 3400 to 3440 cm^{-1} (Ahmad & Benjakul, 2011), suggesting the hydrogen bond coupled with NH group should not contribute significantly to the secondary structure of fish gelatin. Amide I band was found to be associated with the secondary structure of protein (Muyonga et al., 2004). The location of amide I was found to be at 1659 ± 5 cm^{-1} and 1659 ± 7 cm^{-1} for FG and FGS, respectively (Fig. S1C & Table 2), featuring the characteristic of triple helix structure in collagen (Yakimets et al., 2005). While for FGN, amide I was found to be at 1652 ± 7 cm^{-1}, which corresponded to a random coil structure of gelatin (Muyonga et al., 2004).

The changes in peak location and peak height of amide II were similar to that in amide I (Fig. S1E). Amide II also indicates the changes in the secondary structure of gelatin (Barth, 2007); however, this band is usually considered more sensitive to hydration than structural changes of protein (Benjakul, Oungbho, Visessanguan, Thiansilakul, & Roytrakul, 2009). For amide III, the location was not significantly different among all the spectra except at day 10 of storage, where the Amide III band of FGN was shifted to higher wavenumber 1256 ± 14 cm^{-1} than FG and FGS at 1240 ± 0.7 cm^{-1} and 1244 ± 10 cm^{-1}, respectively (Fig. S1G). Because amide III band at 1270 cm^{-1} to 1245 cm^{-1} is associated to the random coil or disordered structure (Cai & Singh, 1999), this result indicates an increased random coil or disordered structure in FGN, especially at day 10.

The addition of NaCl to fish gelatin decreased the peak height of amide A, I, II and III (Fig. S1). In addition, the location of amide I and amide II was shifted to a lower wavenumber by NaCl. The reduction in intensity of amide I, II, III bands by NaCl was associated to the greater loss of molecular order in gelatin (Muyonga et al., 2004). The decreased wavenumber may imply that the changes in the conformation of fish gelatin from helix to random coil decreased the molecular order (Rouhi, Mahmud, Naderi, Ooi, & Mahmood, 2013). The decrease in molecular order of FGN may correlate with the poorer gel textural properties, in particular gel strength, hardness and chewiness as compared to FG and FGS.

3.3.1. Deconvolution of amide I

The mixed secondary structures of protein were presented as several shoulders or components in amide I band (Uriarte-Montoya et al., 2011). Deconvolution of amide I band could enhance the resolution of the peak components, allowing the following curve fitting process to estimate the relative proportion of the components to the overall amide I band (Byler & Susi, 1986).

There were 5 band components identified in amide I region (Fig. S2). There was no significant difference for the location of the each component peaks among samples. When compared with known results, component 1 was imide residue and β-sheet; component 2 was related to the random coil or disordered structure; helical structure was represented by component 3; β-turn structure was associated with component 4 and the presence of component 5 was due to intermolecular association (Barth, 2007; Muyonga et al., 2004).

The percentage accounted by each component is shown in Table 3. The major components for FG and FGS were component 1, 3

Cohesiveness			Chewiness/g			Viscosity/cP		
FG	FGN	FGS	FG	FGN	FGS	FG	FGN	FGS
0.91 ± 0.02^{bC}	0.93 ± 0.01^{aB}	0.93 ± 0.01^{aAB}	1378 ± 256^{abD}	1272 ± 202^{bC}	1484 ± 260^{aC}	12.3 ± 1.2^{aA}	13.0 ± 1.0^{aA}	13.1 ± 1.2^{aA}
0.93 ± 0.02^{aB}	0.93 ± 0.02^{aB}	0.93 ± 0.01^{aAB}	1919 ± 370^{abC}	1801 ± 327^{bB}	2034 ± 322^{aB}	12.0 ± 0.9^{aA}	11.6 ± 0.6^{aB}	11.9 ± 0.9^{aB}
0.93 ± 0.02^{bB}	0.94 ± 0.01^{aAB}	0.94 ± 0.01^{aA}	2018 ± 392^{abBC}	1865 ± 370^{bAB}	2197 ± 407^{aAB}	12.1 ± 0.8^{aA}	11.7 ± 0.6^{aB}	11.7 ± 0.8^{aB}
0.93 ± 0.02^{aB}	0.94 ± 0.02^{aAB}	0.94 ± 0.02^{aA}	2108 ± 256^{abBC}	1917 ± 326^{bAB}	2261 ± 346^{aA}	11.8 ± 1.0^{aA}	11.9 ± 0.6^{aB}	12.1 ± 0.7^{aB}
0.95 ± 0.02^{aA}	0.95 ± 0.01^{aA}	0.94 ± 0.02^{aA}	2106 ± 292^{aBC}	2066 ± 354^{aA}	2199 ± 349^{aAB}	12.2 ± 1.0^{aA}	12.1 ± 0.4^{aB}	12.2 ± 0.5^{aB}
0.92 ± 0.02^{bBC}	0.93 ± 0.01^{aB}	0.93 ± 0.02^{abB}	2214 ± 456^{aAB}	2058 ± 416^{aA}	2201 ± 297^{aAB}	12.2 ± 1.1^{aA}	11.9 ± 0.4^{aB}	12.3 ± 0.6^{aB}
0.93 ± 0.01^{aB}	0.93 ± 0.02^{aB}	0.94 ± 0.02^{aA}	2387 ± 373^{aA}	2084 ± 285^{bA}	2354 ± 314^{aA}	12.4 ± 1.0^{aA}	12.2 ± 0.3^{aB}	12.3 ± 0.7^{aB}

and 5 while the dominant components for FGN were component 1 and 5. The high percentage of component 1 (imide residue or β-sheet) in Nile perch skin and bone gelatin was also observed by Muyonga et al. (2004). This component percentage difference suggested more helical structure existed in FG and FGS than FGN.

The proportion of component 3 in FG, which is associated to helical structure, increased from day 0 to day 10. The increase in helical structure likely occurred at the expense of component 2 (random coil) and 4 (β-turn) as the proportion of these two components decreased from day 0 to day 10. On the contrast, gel

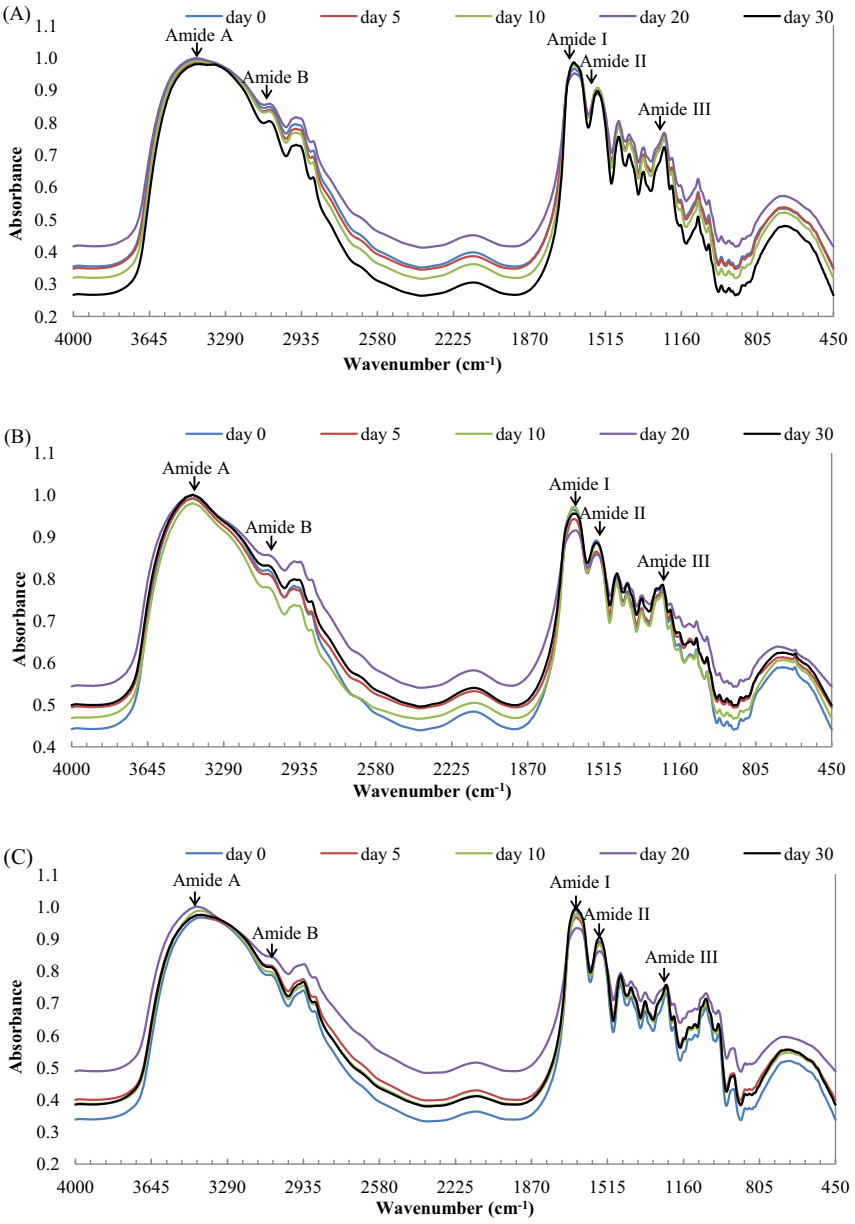

Fig. 1. Averaged and normalized FTIR spectra (A) fish gelatin only (FG); (B) fish gelatin added with 1.5% NaCl (FGN); (C) fish gelatin added with 1.5% sucrose (FGS) over 30 days of storage.

Table 2
Location and assignment of the peaks identified in FTIR spectra.

Region	Peak wavenumber (cm^{-1})			Assignment	References
	FG	FGN	FGS		
Amide A	3411 ± 35^{b}	3435 ± 2^{a}	3413 ± 28^{b}	N–H stretch coupled with H-bond	Sai and Babu (2001)
Amide B	3085 ± 2^{b}	3086 ± 4^{b}	3092 ± 3^{a}	NH bend	Barth (2007)
	2960 ± 4^{a}	2958 ± 9^{a}	2937 ± 6^{b}	CH_2 asymmetical stretch	Abe and Krimm (1972)
	2881 ± 1^{a}	2881 ± 1^{b}	2882 ± 1^{b}	CH_2 symmetrical stretch	Abe and Krimm (1972)
Amide I	1659 ± 5^{a}	1652 ± 7^{b}	1659 ± 7^{a}	C=O stretch/hydrogen bond coupled with COO^{-}	Payne and Veis (1988)
Amide II	1552 ± 3^{a}	1549 ± 4^{b}	1553 ± 3^{a}	NH bend coupled with CN stretch	Jackson, Choo, Watson, Halliday, and Mantsch (1995)
	1453 ± 1^{a}	1453 ± 1^{a}	1453 ± 1^{a}	CH_2 bending	Jackson et al. (1995)
	1400 ± 29^{a}	1405 ± 1^{a}	1405 ± 1^{a}	COO^{-} symmetrical stretch	Jackson et al. (1995)
	1338 ± 1^{a}	1338 ± 7^{a}	1339 ± 1^{a}	CH_2 wag of proline & glycine	Jackson et al. (1995)
Amide III	1241 ± 3^{b}	1246 ± 9^{a}	1241 ± 3^{b}	NH bend stretch coupled CN stretch	Jackson et al. (1995)
Fingerprint	1082 ± 1^{a}	1082 ± 1^{a}	1056 ± 2^{b}	C–O skeletal stretch	Jackson et al. (1995)
	1032 ± 1^{a}	1032 ± 1^{a}	997 ± 1^{b}	C–O skeletal stretch	Staroszczyk, Pielichowska, Sztuka, Stangret, and Kołodziejska (2012)
	974 ± 1^{b}	975 ± 2^{a}	–	C–O skeletal stretch	Jackson et al. (1995)
	938 ± 1^{a}	939 ± 1^{a}	927 ± 2^{b}	C–O skeletal stretch	Jackson et al. (1995)
	874 ± 2^{a}	874 ± 2^{a}	872 ± 1^{b}	Skeletal stretch	Abe and Krimm (1972)
	685 ± 12^{a}	689 ± 15^{a}	677 ± 13^{b}	Skeletal stretch	Abe and Krimm (1972)
	–	622 ± 2^{a}	–	Skeletal stretch	Abe and Krimm (1972)

*Within each peak (row), means with different lowercase letters are significantly different ($P < 0.05$) among different groups.
*The means represented the averaged wavenumber of the peak from the day 0 to day 30 spectra of the same sample (FG, FGN or FGS).
* "–" indicates that the band/peak was absent in the spectra of the sample.

strength of FG increased significantly from day 0 to day 10, supporting that the strengthening effect on the gel by storage time is due to partial renaturation of helix by coil to helix transition. When the storage extended to 20 days and even 30 days, component 1 (β-sheet) increased and replaced helical structure as the dominant component at day 30.

For FGN, it contained less proportion of helix secondary structure than FG and FGS. The hindered formation of helices structure could lead to a weak gelatin gel (Devi, Liu, Hemar, Buckow, & Kasapis, 2013). Moreover, the secondary structure of FGN was consisted of higher proportion of β-sheet and random coil than FG and FGS. The high proportion of random coil structure present in FGN agreed with the high wavenumber of amide III that accompanied with the existence of random coil structure as discussed above.

However, since the assignment of peak components to secondary structure is semi-empirical based on the reported results, the subjective decisions of curve fitting process may further increase errors (Oberg, Ruysschaert, & Goormaghtigh, 2004). In the future, the secondary structure needs to be confirmed, possibly by using circular dichroism.

3.4. AFM

To further understand the underlying mechanism of changed properties by NaCl and sucrose addition, gelatin's nanostrutural analysis was conducted using AFM (Fig. 2 and Fig. 3). In order to study the details at nanoscale, the fish gelatin samples were examined at the original concentration (6.67%, w/w) and diluted 6 times (approximately 1.11%) for the AFM imaging. The summary of

Table 3
Percent area contribution of amide I band component peaks of fish gelatin.

Time (d)	Sample	% Peak area of amide I band's component peaks				
		1	2	3	4	5
0	FG	25.6 ± 1.6^{aB}	9.7 ± 2.2^{bAB}	26.9 ± 2.1^{aBCDE}	9.7 ± 2.2^{bA}	28.1 ± 5.3^{aA}
	FGN	29.8 ± 1.8^{aB}	10.9 ± 2.1^{bAB}	14.5 ± 1.4^{bG}	14.9 ± 1.4^{bA}	29.8 ± 5.3^{aA}
	FGS	26.8 ± 2.5^{aB}	6.8 ± 3.0^{bB}	30.1 ± 6.6^{aBCD}	10.6 ± 2.1^{bA}	25.7 ± 3.8^{aA}
5	FG	27.1 ± 2.0^{bB}	4.9 ± 3.6^{cB}	32.6 ± 1.6^{aABC}	7.5 ± 2.7^{cA}	27.8 ± 1.9^{abA}
	FGN	28.9 ± 2.8^{aB}	6.7 ± 1.7^{cB}	16.2 ± 5.4^{bFG}	12.7 ± 0.3^{bcA}	26.5 ± 4.5^{aA}
	FGS	26.1 ± 4.4^{aB}	7.9 ± 4.6^{cAB}	29.3 ± 6.3^{aBCDE}	14.2 ± 1.8^{bcA}	22.5 ± 4.4^{abA}
10	FG	25.4 ± 2.5^{bB}	2.6 ± 2.4^{cB}	39.1 ± 4.1^{aA}	5.9 ± 0.7^{cA}	27.0 ± 2.8^{bA}
	FGN	31.4 ± 6.3^{aAB}	15.7 ± 6.0^{bA}	16.7 ± 0.9^{bFG}	13.4 ± 2.2^{bA}	27.0 ± 3.0^{aA}
	FGS	26.3 ± 2.3^{bB}	7.1 ± 1.0^{cAB}	34.5 ± 6.5^{aAB}	7.5 ± 0.9^{cA}	24.6 ± 1.7^{bA}
20	FG	32.2 ± 7.9^{aAB}	6.8 ± 6.3^{bB}	26.3 ± 5.2^{aCDE}	5.1 ± 2.9^{bA}	29.7 ± 3.4^{aA}
	FGN	38.0 ± 2.2^{aA}	11.5 ± 7.5^{cAB}	15.6 ± 2.4^{bcG}	11.0 ± 2.1^{cA}	27.4 ± 11.9^{abA}
	FGS	32.6 ± 9.6^{aAB}	10.4 ± 7.8^{cAB}	17.2 ± 6.3^{bcFG}	10.3 ± 1.1^{cA}	29.5 ± 6.6^{abA}
30	FG	29.1 ± 0.7^{aB}	7.0 ± 4.7^{dAB}	21.6 ± 1.3^{bcEFG}	14.8 ± 3.8^{cA}	27.5 ± 2.5^{abA}
	FGN	31.9 ± 3.5^{aAB}	8.1 ± 4.9^{cAB}	24.0 ± 3.1^{bDEF}	9.6 ± 0.6^{cA}	27.8 ± 3.5^{abA}
	FGS	25.1 ± 0.9^{bB}	5.2 ± 2.9^{dB}	33.3 ± 2.6^{aABC}	14.5 ± 3.2^{cA}	21.8 ± 4.4^{bA}

* FG refers to sample contained fish gelatin only, FGN referred to fish gelatin with 1.5% NaCl, FGS indicated fish gelatin added with 1.5% sucrose.
*The average locations of component peak 1 to 5 were 1628 ± 1.7 cm^{-1}, 1647 ± 2.0 cm^{-1}, 1661 ± 2.0 cm^{-1}, 1677 ± 1.7 cm^{-1}, 1695 ± 1.6 cm^{-1}, accordingly.
*Within each row, means with different lowercase letters are significantly different ($P < 0.05$) among different groups. Within each column, means with different capital letters are significantly different among different time points ($P < 0.05$).
*Figures obtained from average of 3 spectra from the triplicate parallel experiments, which each spectrum was the averaged of at least triplicate spectra from one experiments.
* Fit quality of original and fitted Gaussian curve, $R^2 \geq 0.991$.

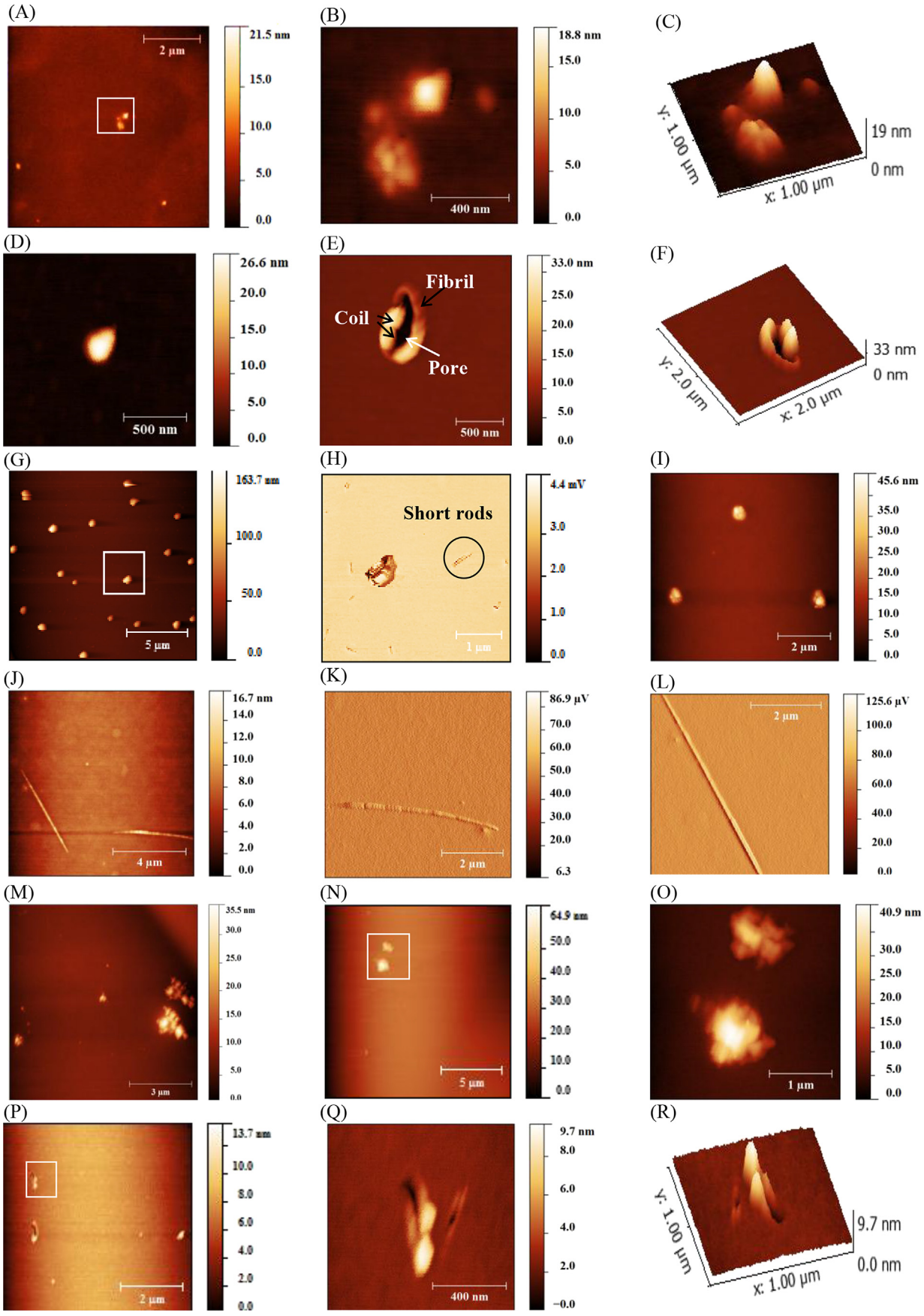

Fig. 2. Nanostructures of diluted fish gelatin (A) typical height images of FG; (B) enlarged region from image (A); (C) 3D image of (B); (D) Spherical aggregates from FG; (E) Ring like structure with pore formation in the center from FG; (F) 3D images of (E); (G) Spherical aggregates from FGN; (H) The error signal mode images showing enlarged region of images (G); (I) Irregular aggregates from FGN; (J) Long rods from FGN; (K) & (L) enlarged error signal mode images of the rods in (J); (M) & (N) typical height images showing aggregates from FGS; (O) enlarged region of image (N); (P) Ring like structure of FGS; (Q) enlarged region of images (P); (R) 3D images of image (Q).

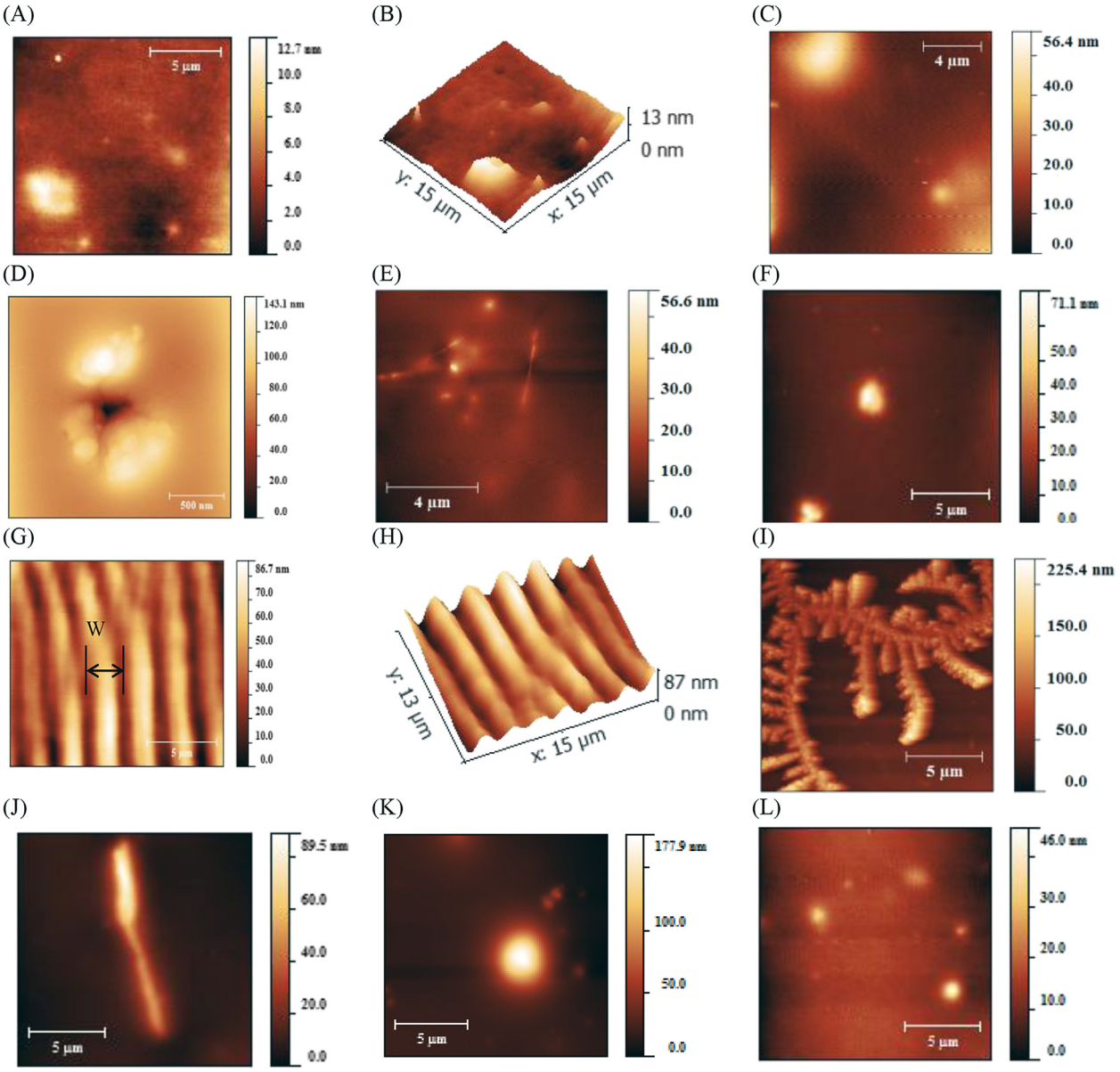

Fig. 3. Nanostructure of fish gelatin solution at 6.67% (w/w), (A) Large irregular aggregates and continuous rough surface from fish gelatin only (FG); (B) 3D image of (A); (C) large spherical aggregates from FG; (D) Irregular aggregates and pore structure from fish gelatin added with 1.5% NaCl (FGN); (E) Rods like structure from FGN; (F) Irregular and spherical aggregates from FGN; (G) Continuous fibre network from FGN; (H) 3D image of (G); (I) Fractal tree pattern from FGN; (J) Long rods from fish gelatin added with 1.5% sucrose (FGS); (K) & (L) Spherical aggregates from FGS. W: width of the main chain of fibre network.

Table 4
Summary of the nanostructure present in the fish gelatin (FG), fish gelatin with addition of 1.5% NaCl (FGN), fish gelatin with addition of 1.5% sucrose (FGS). "+" indicates the structure is present in the sample,"−" indicates the structure was absence in the sample.

Nanostructure	1.11% Gelatin			6.67% Gelatin			References
	FG	FGN	FGS	FG	FGN	FGS	
Spherical aggregates	+	+	+	+	+	+	Yang, Wang, Regenstein, et al. (2007)
Irregular aggregates	+	+	+	+	+	+	Yang, Wang, Regenstein, et al. (2007)
Ring like structure[a]	+	−	+	−	−	−	Yang, Wang, Regenstein, et al. (2007)
Rod like structure[b]	−	+	−	−	+	+	Farris et al. (2011), Mackie et al. (1998)
Pore	+	−	+	−	+	−	Yang, Wang, Regenstein, et al. (2007)
Fractal Tree pattern	−	−	−	−	+	−	Mohanty and Bohindar (2005)
Continuous fibre network	−	−	−	−	+	−	Yang and Wang (2009)

[a] Ring like structure referred to the fibre/coil structure reported by Yang, Wang, Regenstein, et al. (2007).
[b] Rod like structure referred to the fibre or triple helix bundles reported in Farris et al. (2011) & Mackie et al. (1998).

Table 5
Effect of solute addition on the dimension of spherical aggregates.

Sample	Diameter (nm)		Height (nm)	
	1.11% Gelatin	6.67 %Gelatin	1.11% Gelatin	6.67% Gelatin
FG	201 ± 115^{d}	1050 ± 730^{b}	23.8 ± 43.1^{b}	21.0 ± 19.9^{b}
FGN	492 ± 253^{c}	1163 ± 836^{b}	44.0 ± 41.8^{a}	34.9 ± 34.8^{a}
FGS	212 ± 126^{d}	1419 ± 1075^{a}	8.8 ± 6.5^{c}	23.1 ± 35.1^{b}

*FG is the control sample contained fish gelatin only, FGN is the fish gelatin sample added with 1.5% NaCl, FGS is the fish gelatin sample added with 1.5% sucrose.
*The replication numbers for 1.11% gelatin groups were 49, 43 and 112 for FG, FGN and FGS, respectively while for 6.67% gelatine they were 101, 48 and 48, respectively.
*Means with different letters within the same main column (diameter or height) are significantly different ($P < 0.05$).

the nanostructures was shown in Table 4. Overall, various nanostructures were present, indicating the heterogeneity of fish gelatin.

In more details, there were ring like structures (Fig. 2E and P), which were consisted of spherical aggregate region that was coil structure, and a narrower chain like region which was considered as fibril structure (Yang, Wang, Regenstein, et al., 2007). The presence of this structure indicated the multimeric association process of gelatin (Yang, Wang, Regenstein, et al., 2007). The formation process of pore at the centre of the ring like structure was similar to that of the annular pore structure (Yang, Wang, Regenstein, et al., 2007, Yang, Wang, Zhou, Regenstein, 2008). In general, the formation of pore was less frequently observed than the compact sphere.

After gelatin was diluted 6 times, large spherical aggregates started to be observed in the sample added with 1.5% NaCl as shown in Fig. 2G to I. This result was similar to the observation of 1% w/v of type B bovine gelatin with 0.1 M NaCl Mohanty & Bohindar (2005). Gelatin is a polyelectrolyte, addition of NaCl promoted electrostatic interactions of the charged segments in gelatin, yielding small intramolecular aggregates at size of 30 ± 5 nm. Due to intermolecular aggregates, larger particles size may also be observed with an average radius at about 200 nm (Mohanty & Bohindar, 2005). The intermolecular aggregates occurred when different molecules of gelatin were crosslinked and participated in the formation of parallel pattern triple helices, while intramolecular crosslinkingof gelatin molecule led to reversed fold pattern. The occurrence of different types of interaction depended on the factors including concentration of gelatin and temperature (Harrington & Rao, 1970). In addition to the large spherical aggregates, short rods were also observed at the background of Fig. 2G and highlighted in Fig. 2H. Those structures were explained as triple helix bundles of gelatin (Mackie, Gunning, Ridout, & Morris, 1998). The average length of the short rods was 393.34 ± 192.16 nm, while the height was 3.78 ± 0.63 nm. These results were similar to those observed by Farris et al. (2011), where the length was 200–600 nm and the height was at about 6 nm. Mackie et al. (1998) also observed the similar structure at length from 100 to 500 nm and height at 1–8.5 nm. In addition to the short rod structure, long rod like structures were also found (Fig. 2J, K, L and Fig. 3E and J). From the enlarged error signal mode image of the long rods (Fig. 2K and L), this structure seemed to consist of several segments that joined together, indicating that individual aggregates could join and lead to the growth of the long rods.

Besides, large aggregates were observed in FG and FGS but the aggregates in FGS were more spherical (Fig. 3K and L). On the contrast, more irregular aggregates were observed in FG (Fig. 3A and C). In addition to irregular aggregates, continuous rough

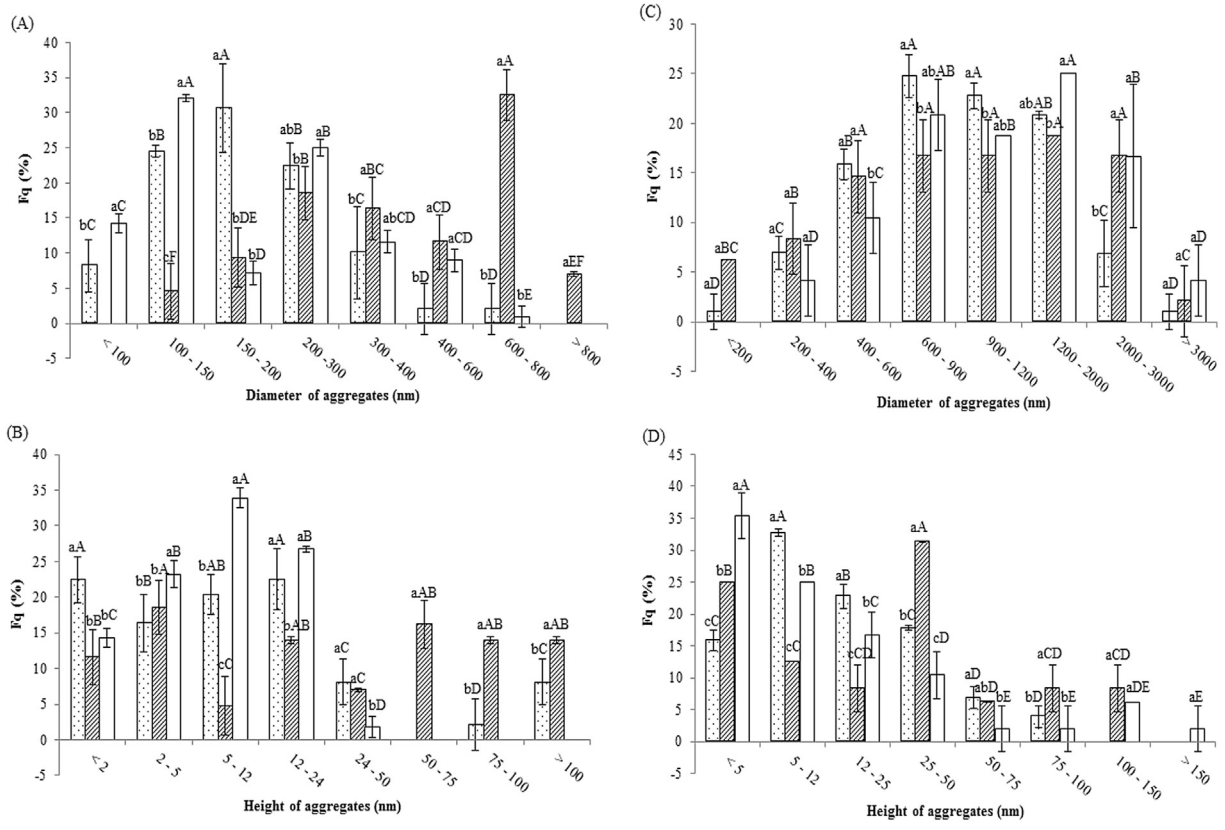

Fig. 4. Frequency histrogram for the diameters and heights of spherical aggregates of fish gelatin (FG,□), fish gelatin added with 1.5% NaCl (FGN, ▨) and fish gelatin added with 1.5% Sucrose (FGS, □) (A) & (B) diluted gelatin solution; (C) & (D) 6.67% gelatin solution*. *Within each dimension, means with different lowercase letters are significantly different among different groups ($P < 0.05$). Within each group, means with different capital letters are significantly different among different dimension ($P < 0.05$).

surface was also observed in FG (Fig. 3A), which was similar to the surface of fish gelatin film with sorbitol and glycerol as plasticiser (Rouhi et al., 2013).

Interestingly, a unique fractal tree pattern was observed at a random basis only in FGN (Fig. 3I). Fractal is a self-similar structure. Addition of metal salt such as NaCl in protein could change aggregates' appearance and increased fractal dimension as a result of aggregate restructuring (Kumagai, Matsunaga, & Hagiwara, 1999). This feature structure may be formed due to diffusion-limited aggregation process during gelatin dehydration on the mica surface and individual aggregates swarming and joining together in specific orientation Mohanty and Bohindar (2005). Another unique nanostructure was the continuous fibre network observed only in FGN (Fig. 3G), with the width of the main chain about 2.51 ± 0.48 μm. This fibre structure was similar to that reported by Yang and Wang (2009) with gelatin at 3.33% and 6.67%. The fibre network is believed to be assembles from individual fibril of triple helix bundles, which occurs during gelation (Yang & Wang, 2009).

In our study, the most frequently observed morphology from AFM was spherical aggregates. It was found that formation of aggregates was influence by hydrogen bond while the diameter of aggregates was influence by hydrophobic interaction (Duconseille, Astruc, Quintana, Meersman, & Sante-Lhoutellier, 2014). Dimension of spherical aggregates were quantified in Table 5. When the solution was diluted, the diameter of aggregates decreased but the height of diameter was not significantly changed. Increasing gelatin concentration enhanced hydrophobic interaction between gelatin chains, leading to formation of large aggregates (Duconseille et al., 2014) or dense structure (Pang, Deeth, Sopade, Sharma, & Bansal, 2014). For diluted gelatin, the diameter of spherical aggregates showed a negative correlation to the gel strength. For example, the aggregates of FGN were the largest while the gel strength was the lowest among the three sample groups. A similar trend of diameter was observed for the average height of the aggregates. This phenomenon may be caused by the increase in electrolyte concentration due to NaCl addition, which resulted in reduced thickness of the diffuse double layer at the surface of gelatin. Thus electrostatic potentials reduced quickly with distance, and gelatin became more prone to aggregate resulting in larger aggregates (Yakhno, 2008).

Compared to nano-aggregates found in AFM, results from FTIR revealed that gelatin contained helices as one of the major component in FG and FGS. It should be noted that the two techniques investigated the structure from different levels and based on different mechanisms. The basis of FTIR secondary structural analysis was based on conformation sensitivity of IR spectra (Surewicz, Mantsch, & Chapman, 1993), while AFM observed the morphology of gelatin. Individual triple helix could be difficult to detect in AFM due to aggregation of gelatin on mica sheet. It was reported that only bundles of triple helices were observed by AFM (Mackie et al., 1998; Yang & Wang, 2009). However, both FTIR and AFM methods confirmed the presence of heterogeneous structures in fish gelatin. In addition, the influence of NaCl addition on the structure of fish gelatin can be investigated by both methods.

As shown in Fig. 4A and B, the frequency distribution of diameter and height of the diluted FGN samples were shifted to greater dimension when NaCl was added into fish gelatin. Specifically, the diameters of aggregates were between 134 and 931 nm, with most of them falling within the range of 600–800 nm. The height distribution among FGN was much widespread from 1.07 to 132 nm. In comparison, most of the particles in FG and FGS were less than 24 nm height. As a contrast, the average diameter of aggregates from catfish skin gelatin was about 267 ± 131 nm (Yang, Wang, Regenstein, et al., 2007), while the size of bovine and porcine gelatin nanoparticle was about 180 ± 42 nm (Saxena, Sachin, Bohidar, & Verma, 2005), and the aggregates around 100–219 nm were found in gelatin extracted from skin, muscle and bone of marine cornet fish (Nazeer & Kavya Deepthi, 2013). All these aggregates were similar in diameter to those observed in diluted fish gelatin here. Large aggregates were less different among samples since they were found in all samples at 6.67%, Moreoever, the distribution of diameter and height were more even in 6.67% gelatin than those in diluted sample, histogram in Fig. 4C and D. From these results, the correlation of the aggregate dimension to physical properties of gelatin was difficult to determine with gelatin at 6.67%.

It should be noted that the dimension quantified from AFM image has limitation partially due to the probe broadening effect (Yang, Wang, Regenstein, et al., 2007). Despite the absence of continuous fibre network in FG and FGN, the dimension results of spherical aggregates, especially those in the diluted samples indicated that the addition of NaCl favoured formation of large aggregates. The unique fractal tree pattern also suggested the possibility of salting out effect because of addition of NaCl. This type of aggregation in FGN could be unfavourable for the formation of a strong 3D network, leading to poorer textural properties.

4. Conclusions

Addition of salt (NaCl) into fish gelatin reduced gel strength and textural properties, while the addition of sucrose at 1.5% did not affect these properties significantly. Viscosity of gelatin remained stable and unaffected by solute addition and storage period. In general, physical properties of fish gelatin maintained stable physical properties up to at least 30 days of cold storage. Addition of 1.5% NaCl led to the loss of molecular order and lower helix and higher random coil/disordered structure. The overall changes in secondary structure by sodium chloride addition led to the poor textural properties of fish gelatin. AFM study demonstrated the heterogeneous nanostructure of fish gelatin. Although large aggregates were observed in all samples, addition of NaCl favoured formation of large aggregates, while might be unfavourable for the formation of a rigid gel network. Interestingly, the continuous fibre network was only observed when NaCl was added. These results suggest that electrostatic interaction might be important to the structure of fish gelatin as shown by the dependence of textural properties and structure of fish gelatin on the addition of NaCl.

Acknowledgements

We acknowledge the financial support by Singapore Ministry of Education Academic Research Fund Tier 1 (R-143-000-583-112) and the start-up grant (R-143-000-561-133) by National University of Singapore. Projects 31371851, 31471605, 31071617 and 31200801 supported by NSFC and Natural Science Foundation of Jiangsu Province (BK20141220) also contributed to this research.

Appendix A. Supplementary data

Supplementary data related to this article can be found at http://dx.doi.org/10.1016/j.foodhyd.2014.10.021.

References

Abe, Y., & Krimm, S. (1972). Normal vibrations of crystalline polyglycine I. *Biopolymers, 11*, 1817–1839.
Ahmad, M., & Benjakul, S. (2011). Characteristics of gelatin from the skin of unicorn leatherjacket (*Aluterus monoceros*) as influenced by acid pretreatment and extraction time. *Food Hydrocolloids, 25*, 381–388.
Arnesen, J. A., & Gildberg, A. (2007). Extraction and characterisation of gelatine from Atlantic salmon (*Salmo salar*) skin. *Bioresource Technology, 98*, 53–57.
Barth, A. (2007). Infrared spectroscopy of proteins. *Biochimica et Biophysica Acta (BBA) - Bioenergetics, 1767*, 1073–1101.

Benjakul, S., Oungbho, K., Visessanguan, W., Thiansilakul, Y., & Roytrakul, S. (2009). Characteristics of gelatin from the skins of bigeye snapper, *Priacanthus tayenus* and *Priacanthus macracanthus*. *Food Chemistry, 116*, 445–451.

Byler, D. M., & Susi, H. (1986). Examination of the secondary structure of proteins by deconvolved FTIR spectra. *Biopolymers, 25*, 469–487.

Cai, S., & Singh, B. R. (1999). Identification of β-turn and random coil amide III infrared bands for secondary structure estimation of proteins. *Biophysical Chemistry, 80*, 7–20.

Choi, S. S., & Regenstein, J. M. (2000). Physicochemical and sensory characteristics of fish gelatin. *Journal of Food Science, 65*, 194–199.

Choi, Y. H., Lim, S. T., & Yoo, B. (2004). Measurement of dynamic rheology during ageing of gelatine–sugar composites. *International Journal of Food Science & Technology, 39*, 935–945.

Devi, A. F., Liu, L. H., Hemar, Y., Buckow, R., & Kasapis, S. (2013). Effect of high pressure processing on rheological and structural properties of milk–gelatin mixtures. *Food Chemistry, 141*, 1328–1334.

Díaz-Calderón, P., Caballero, L., Melo, F., & Enrione, J. (2014). Molecular configuration of gelatin–water suspensions at low concentration. *Food Hydrocolloids, 39*, 171–179.

Duconseille, A., Astruc, T., Quintana, N., Meersman, F., & Sante-Lhoutellier, V. (2014). Gelatin structure and composition linked to hard capsule dissolution: a review. *Food Hydrocolloids*. http://dx.doi.org/10.1016/j.foodhyd.2014.06.006.

Farris, S., Schaich, K. M., Liu, L., Cooke, P. H., Piergiovanni, L., & Yam, K. L. (2011). Gelatin–pectin composite films from polyion-complex hydrogels. *Food Hydrocolloids, 25*, 61–70.

Feng, X., Lai, S., & Yang, H. (2014). Sustainable seafood processing: utilisation of fish gelatin. *Austin Journal of Food Science, 2*, 1–2.

Garrigues, J. M., Akssira, M., Rambla, F. J., Garrigues, S., & de la Guardia, M. (2000). Direct ATR-FTIR determination of sucrose in beet root. *Talanta, 51*, 247–255.

Giménez, B., Turnay, J., Lizarbe, M. A., Montero, P., & Gómez-Guillén, M. C. (2005). Use of lactic acid for extraction of fish skin gelatin. *Food Hydrocolloids, 19*, 941–950.

Gudmundsson, M. (2002). Rheological properties of fish gelatins. *Journal of Food Science, 67*, 2172–2176.

Gudmundsson, M., & Hafsteinsson, H. (1997). Gelatin from cod skins as affected by chemical treatments. *Journal of Food Science, 62*, 37–39.

Harrington, W. F., & Rao, N. V. (1970). Collagen structure in solution. I. Kinetics of helix regeneration in single-chain gelatins. *Biochemistry, 9*, 3714–3724.

Haug, I. J., Draget, K. I., & Smidsrød, O. (2004). Physical and rheological properties of fish gelatin compared to mammalian gelatin. *Food Hydrocolloids, 18*, 203–213.

Jackson, M., Choo, L.-P., Watson, P. H., Halliday, W. C., & Mantsch, H. H. (1995). Beware of connective tissue proteins: assignment and implications of collagen absorptions in infrared spectra of human tissues. *Biochimica et Biophysica Acta (BBA) – Molecular Basis of Disease, 1270*, 1–6.

Jamilah, B., & Harvinder, K. G. (2002). Properties of gelatins from skins of fish—black tilapia (*Oreochromis mossambicus*) and red tilapia (*Oreochromis nilotica*). *Food Chemistry, 77*, 81–84.

Johnston-Banks, F. A. (1990). Gelatine. In P. Harris (Ed.), *Food gels* (pp. 233–289). Springer.

Kaewruang, P., Benjakul, S., Prodpran, T., Encarnacion, A. B., & Nalinanon, S. (2014). Impact of divalent salts and bovine gelatin on gel properties of phosphorylated gelatin from the skin of unicorn leatherjacket. *LWT – Food Science and Technology, 55*, 477–482.

Karim, A. A., & Bhat, R. (2009). Fish gelatin: properties, challenges, and prospects as an alternative to mammalian gelatins. *Food Hydrocolloids, 23*, 563–576.

Koli, J. M., Basu, S., Nayak, B. B., Kannuchamy, N., & Gudipati, V. (2011). Improvement of gel strength and melting Point of fish gelatin by addition of coenhancers using response surface methodology. *Journal of Food Science, 76*, E503–E509.

Kumagai, H., Matsunaga, T., & Hagiwara, T. (1999). Effect of salt addition on the fractal structure of aggregates formed by heating dilute BSA solutions. *Bioscience, Biotechnology, and Biochemistry, 63*, 223–225.

Mackie, A. R., Gunning, A. P., Ridout, M. J., & Morris, V. J. (1998). Gelation of gelatin observation in the bulk and at the air-water interface. *Biopolymers, 46*, 245–252.

Mohanty, B., & Bohindar, H. B. (2005). AFM study of morphology of ethanol induced gelatin coacervation. *International Journal of Polymeric Materials and Polymeric Biomaterials, 54*, 675–689.

Muyonga, J. H., Cole, C. G. B., & Duodu, K. G. (2004). Fourier transform infrared (FTIR) spectroscopic study of acid soluble collagen and gelatin from skins and bones of young and adult Nile perch (*Lates niloticus*). *Food Chemistry, 86*, 325–332.

Nazeer, R. A., & Kavya Deepthi, M. (2013). Physicochemical and nanostructural properties of gelatin from uneconomical marine cornet fish (*Fistularia petimba*). *Food Science and Biotechnology, 22*, 9–14.

Oberg, K. A., Ruysschaert, J.-M., & Goormaghtigh, E. (2004). The optimization of protein secondary structure determination with infrared and circular dichroism spectra. *European Journal of Biochemistry, 271*, 2937–2948.

Pang, Z., Deeth, H., Sopade, P., Sharma, R., & Bansal, N. (2014). Rheology, texture and microstructure of gelatin gels with and without milk proteins. *Food Hydrocolloids, 35*, 484–493.

Payne, K. J., & Veis, A. (1988). Fourier transform ir spectroscopy of collagen and gelatin solutions: deconvolution of the amide I band for conformational studies. *Biopolymers, 27*, 1749–1760.

Rouhi, J., Mahmud, S., Naderi, N., Ooi, C., & Mahmood, M. (2013). Physical properties of fish gelatin-based bio-nanocomposite films incorporated with ZnO nanorods. *Nanoscale Research Letters, 8*, 1–6.

Sai, K. P., & Babu, M. (2001). Studies on Rana tigerina skin collagen. *Comparative Biochemistry and Physiology Part B: Biochemistry and Molecular Biology, 128*, 81–90.

Sarabia, A. I., Gomez-Guillen, M. C., & Montero, P. (2000). The effect of added salts on the viscoelastic properties of fish skin gelatin. *Food Chemistry, 70*, 71–76.

Saxena, A., Sachin, K., Bohidar, H. B., & Verma, A. K. (2005). Effect of molecular weight heterogeneity on drug encapsulation efficiency of gelatin nano-particles. *Colloids and Surfaces B: Biointerfaces, 45*, 42–48.

Staroszczyk, H., Pielichowska, J., Sztuka, K., Stangret, J., & Kołodziejska, I. (2012). Molecular and structural characteristics of cod gelatin films modified with EDC and TGase. *Food Chemistry, 130*, 335–343.

Surewicz, W. K., Mantsch, H. H., & Chapman, D. (1993). Determination of protein secondary structure by Fourier transform infrared spectroscopy: a critical assessment. *Biochemistry, 32*, 389–394.

Uriarte-Montoya, M. H., Santacruz-Ortega, H., Cinco-Moroyoqui, F. J., Rouzaud-Sández, O., Plascencia-Jatomea, M., & Ezquerra-Brauer, J. M. (2011). Giant squid skin gelatin: chemical composition and biophysical characterization. *Food Research International, 44*, 3243–3249.

USDA. (2013). *USDA National Nutrient Database for Standard Reference*. Release 26.

Yakhno, T. (2008). Salt-induced protein phase transitions in drying drops. *Journal of Colloid and Interface Science, 318*, 225–230.

Yakimets, I., Wellner, N., Smith, A. C., Wilson, R. H., Farhat, I., & Mitchell, J. (2005). Mechanical properties with respect to water content of gelatin films in glassy state. *Polymer, 46*, 12577–12585.

Yang, H., & Wang, Y. (2009). Effects of concentration on nanostructural images and physical properties of gelatin from channel catfish skins. *Food Hydrocolloids, 23*, 577–584.

Yang, H., Wang, Y., Jiang, M., Oh, J., Herring, J., & Zhou, P. (2007). 2-step optimization of the extraction and subsequent physical properties of channel catfish (*Ictalurus punctatus*) skin gelatin. *Journal of Food Science, 72*, C188–C195.

Yang, H., Wang, Y., Regenstein, J. M., & Rouse, D. B. (2007). Nanostructura characteization of catfish skin gelatin using atomic force microscopy. *Journal of Food Science, 72*, C430–C440.

Yang, H., Wang, Y., Zhou, P., & Regenstein, J. M. (2008). Effects of alkaline and acid pretreatment on the physical properties and nanostructures of the gelatin from channel catfish skins. *Food Hydrocolloids, 22*, 1541–1550.

Zhang, F., Xu, S., & Wang, Z. (2011). Pre-treatment optimization and properties of gelatin from freshwater fish scales. *Food and Bioproducts Processing, 89*, 185–193.

Zhou, P., Mulvaney, S. J., & Regenstein, J. M. (2006). Properties of Alaska pollock skin gelatin: a comparison with tilapia and pork skin gelatins. *Journal of Food Science, 71*, C313–C321.